

The complex exposure histories of the Pitts and Horse Creek iron meteorites: Implications for meteorite delivery models

K. C. WELTEN^{1*}, K. NISHIIZUMI¹, B. LAVIELLE², M. W. CAFFEE^{3,4}, D. J. HILLEGONDS³,
R. C. FINKEL³, D. KOLLAR⁵, and J. MASARIK⁵

¹Space Sciences Laboratory, University of California, Berkeley, California 94720–7450, USA

²URA 451 of CNRS, Centre d'Etudes Nucleaires de Bordeaux-Gradignan, Université de Bordeaux I,
BP 120, 33175 Gradignan Cedex, France

³CAMS, Lawrence Livermore National Laboratory, Livermore, California 94550, USA

⁴Present address: Department of Physics, Purdue University, West Lafayette, Indiana 47907, USA

⁵Nuclear Physics Department, Comenius University, SK-842 15 Bratislava, Slovakia

*Corresponding author. E-mail: kcwelten@berkeley.edu

(Received 11 June 2007; revision accepted 10 February 2008)

Abstract—The concentrations of cosmogenic radionuclides and noble gases in Pitts (IAB) and Horse Creek (ungrouped) provide unambiguous evidence that both irons have a complex exposure history with a first-stage irradiation of 100–600 Myr under high shielding, followed by a second-stage exposure of ~1 Myr as small objects. The first-stage exposure ages of ~100 Myr for Horse Creek and ~600 Myr for Pitts are similar to cosmic-ray exposure ages of other iron meteorites, and most likely represent the Yarkovsky orbital drift times of irons from their parent bodies in the main asteroid belt to one of the nearby chaotic resonance zones. The short second-stage exposure ages indicate that collisional debris from recent impact events on their precursor objects was quickly delivered to Earth. The short delivery times suggests that the recent collision events occurred while the precursor objects of Horse Creek and Pitts were either very close to the chaotic resonance zones or already in Earth-crossing orbits. Since the cosmogenic noble gas records of Horse Creek and Pitts indicate a minimum radius of a few meters for the precursor objects, but do not exclude km-sized objects, we conclude that these irons may represent fragments of two near-Earth asteroids, 3103 Eger and 1986 DA, respectively. Finally, we used the cosmogenic nuclide concentrations in Horse Creek, which contains 2.5 wt% Si, to test current model calculations for the production of cosmogenic ¹⁰Be, ²⁶Al, and neon isotopes from iron, nickel, and silicon.

INTRODUCTION

The cosmic-ray exposure (CRE) age of a meteorite measures the time it has been exposed to cosmic rays, either on or near the surface of its parent body and/or as a small (meter-sized) object in space. It is usually assumed that meteorites were ejected from shielded positions on their parent body and received all of their CRE as small objects in space. If so, the CRE ages simply represent the delivery times from their parent bodies in the asteroid belt to Earth. While stony meteorites have typical CRE ages between 1–100 Myr, most iron meteorites show ages in the range of 100 Myr to 1 Gyr (Voshage and Feldman 1979; Voshage et al. 1983). The long CRE ages of iron meteorites have generally been attributed to the longer collisional lifetime of irons, which have higher physical strength than stones (Farinella et al. 1998). However, the long

CRE ages of iron meteorites also imply that irons have longer “storage times” in the asteroid belt than stones (Gladman et al. 1997). These long storage times are now understood in the framework of the Yarkovsky effect (Rubincam 1995), which predicts very slow orbital drift rates for irons relative to those of stones (Farinella et al. 1998; Hartmann et al. 1999; Bottke et al. 2000). The delivery of meteorites from the asteroid belt to Earth thus involves two steps: a slow mechanism driven by the Yarkovsky effect which gradually moves meter- to km-sized collisional fragments from their parent bodies in the asteroid belt to one of the orbital resonances. This step is followed by a fast and chaotic mechanism, caused by the gravitational pull of Jupiter, which increases the orbital eccentricity of meteoroids injected into these orbital resonances, delivering a small fraction to Earth within a few Myr (Wetherill 1985; Gladman et al. 1997).

A small fraction of meteorites shows unambiguous evidence of complex exposure histories, i.e., irradiation under two (or more) different shielding conditions due to collisional breakup events. For chondrites, complex exposure histories were first found in Antarctic meteorites (Nishiizumi et al. 1979), followed by Jilin (Honda et al. 1982) and several others (cf. Herzog et al. 1997; Welten et al. 2003). Many of these complex exposure histories involve a relatively short second stage of <1 Myr, leading to undersaturation of the long-lived radionuclides, such as ^{53}Mn , ^{10}Be , and ^{26}Al , while the stable noble gas revealed much longer exposure ages.

Several large iron meteorites, including Canyon Diablo (Heymann et al. 1966), Sikhote Alin (Vilcsek and Wänke 1961), and Odessa (Herzog et al. 1976) also show evidence of complex exposure histories. However, the second stage exposure ages of these irons are estimated at 75–200 Myr and are not as well constrained as those of stone meteorites with complex exposure histories. On the other hand, iron meteorites with short CRE ages (<100 Myr) are rare and have not been studied in much detail. One of the reasons is that ~75% of the available iron meteorite ages were determined using the ^{41}K - ^{40}K method, which has a typical uncertainty of ~100 Myr (Voshage and Feldman 1979). Therefore, iron meteorites with low concentrations of cosmogenic noble gases were generally not selected for the ^{41}K - ^{40}K exposure age studies. At least 10 iron meteorites, mostly IIAB and IIE irons, were reported to have CRE ages <100 Myr (e.g., Lavielle et al. 1985). However, it is not clear how many of these low ages are due to complex exposure histories, since it often takes several cosmogenic radionuclides and noble gases to detect a complex exposure history. The short CRE ages include ~7 Myr for the ungrouped iron Rafrüti (Terribilini et al. 2000), ~8 Myr for Watson (IIE; Olsen et al. 1994), ~9 Myr for Braunau (IIA; Cobbs 1966; Chang and Wänke 1969) and ~15 Myr for Kodaikanal (IIE; Bogard et al. 1969) and Bahjoi (IAB; Cobbs 1966). The identification of irons with either CRE ages <5 Myr or with complex CRE histories with a short second stage, would be interesting, since this could point at a dynamic link of these irons to the small (~2 km) Earth-approaching M-type asteroid 1986 DA, which is believed to be composed of metallic FeNi (Tedesco and Gradie 1987; Ostro et al. 1991).

In this work we investigate the CRE history of two iron meteorites, Pitts (IAB) and Horse Creek (ungrouped). Begemann et al. (1970) concluded, based on cosmogenic noble gas and ^{36}Cl concentrations, that the Pitts meteorite has a complex exposure history characterized by a first stage of 20–60 Myr under high shielding conditions, followed by a second stage of <0.3 Myr under low shielding conditions. No previous cosmogenic nuclide data were available for Horse Creek, which was not specifically selected for this study. However, when preliminary radionuclide results showed it had a recent exposure history similar to that of Pitts, we included it in this work. To reconstruct the exposure history of

Pitts and Horse Creek, we measured concentrations of the cosmogenic radionuclides ^{10}Be , ^{26}Al , ^{36}Cl , and ^{41}Ca as well as cosmogenic noble gases in both irons. The measured concentrations were interpreted using calculated production rates based on the LAHET (Los Alamos High Energy Transport) Code System (LCS) (Masarik and Reedy 1994; Masarik et al. 2001), as well as empirical correlations for the noble gas and radionuclide production rate ratios (Voshage and Feldmann 1979; Honda et al. 2002). We will reconstruct the exposure histories of Horse Creek and Pitts and discuss their implications for meteorite delivery models.

EXPERIMENTAL METHODS

Meteorite Samples

Pitts fell in 1921 as a small shower in Georgia, USA; four fragments totaling ~3.8 kg in mass were recovered. It is classified as a IAB iron with silicate inclusions (Buchwald 1975; Grady 2000). We received a sample from the same ~1.2 kg fragment (USNM 1378) from which the sample studied by Begemann et al. (1970) was obtained, although the relative positions of the two samples is unknown.

Horse Creek is a 570 g iron meteorite, found in (or before) 1937 in Colorado, USA. It is classified as an anomalous iron (e.g., Buchwald 1975), although it is listed as a mesosiderite in *Catalogue of meteorites* (Grady 2000). Horse Creek is composed mainly of Si-bearing metal (2.5 wt% Si in the kamacite), which contains traces of perryite, $(\text{Fe}, \text{Ni})_x\text{Si}_y$, but has no silicates. The presence of perryite and Si in the metal, as well as the trace element abundances, suggest that Horse Creek is related to metal-containing aubrites (enstatite achondrites), such as Mt. Egerton and Norton County (Wasson and Wai 1970; Casanova et al. 1993). The latter argue that the approximately chondritic siderophile element abundances in Horse Creek exclude the possibility that it represents the differentiated core of the aubrite parent body. Instead, they propose that the Horse Creek iron as well as metal nodules found in Norton County and other aubrites represent the metal that, during partial melting on the aubrite parent body, was not completely segregated from the silicates. Partly due to the unknown fall location and circumstances, it is not clear if the Horse Creek iron entered the Earth's atmosphere as an iron meteoroid or as an unusually large metal nodule inside an aubritic meteoroid.

Radionuclides

The samples were ultrasonically agitated in 0.2N HCl, followed by leaching in concentrated HF to remove troilite and silicate inclusions. The metal samples, 133.4 mg of Pitts and 350.0 mg of Horse Creek, were dissolved in 1.5 N HNO_3 , along with a carrier solution containing Be, Al, Cl, and Ca.

After taking an aliquot for chemical analysis by atomic absorption spectrometry (Table 1a), Cl was isolated as AgCl. Our standard procedures were used to separate Be, Al and Ca; these procedures use anion exchange chromatography, acetylacetone solvent extraction, and cation exchange chromatography techniques. The separated fractions of Be, Al, Cl, and Ca were further purified and converted to BeO, Al₂O₃, AgCl, and CaF₂ for accelerator mass spectrometry (AMS) measurements at the Lawrence Livermore National Laboratory AMS facility (Davis et al. 1990). After making corrections for background and chemical blanks, the measured ratios were normalized to AMS standards (Nishiizumi et al. 2000, 2007; Sharma et al. 1990; Nishiizumi 2004). We used half lives of 1.04×10^5 yr for ⁴¹Ca, 3.01×10^5 yr for ³⁶Cl, 7.05×10^5 yr for ²⁶Al, and a new half-life of 1.36×10^6 yr for ¹⁰Be (Nishiizumi et al. 2007). The results of the AMS measurements are shown in Table 1b. The quoted errors include 1 σ uncertainties in the measured ratios of samples, standards and blanks, but not the uncertainties in the absolute values of the AMS standards.

Noble Gases

The metal samples were ultrasonically cleaned in 10% HNO₃ to remove terrestrial atmospheric gases. Measurements of He, Ne, and Ar were performed using a V. G. Micromass 1202 mass spectrometer (Lavielle et al. 1999). The noble gas results reported in Table 2 have typical precisions (2 σ) of 1–4% in the absolute gas concentrations, and of 0.5–1.0% in the isotope ratios. The measured ²⁰Ne/²²Ne ratio of 1.00 in Pitts indicates a small contribution of atmospheric Ne, whereas the ²⁰Ne/²²Ne ratio of 0.81 in Horse Creek indicates that neon in this meteorite is entirely cosmogenic. Corrections for atmospheric ³⁶Ar and ³⁸Ar were made based on the measured ⁴⁰Ar concentration and atmospheric ⁴⁰Ar/³⁶Ar and ³⁶Ar/³⁸Ar ratios of 296 and 5.32, respectively.

RESULTS AND DISCUSSION

Pitts

The measured ⁴¹Ca concentration of 21.2 ± 1.3 dpm/kg in Pitts is nearly equal to the expected saturation value of 24 ± 1 dpm/kg in iron meteorites with small pre-atmospheric sizes (Fink et al. 1991), thus constraining its pre-atmospheric radius to less than ~20 cm. The recovered mass of ~3.8 kg is consistent with a small pre-atmospheric size. In contrast, the concentrations of ²⁶Al and ¹⁰Be are a factor of 2–4 lower than the production rates of these nuclides in small iron meteorites (Aylmer et al. 1988; Lavielle et al. 1999). Since the production rate ratio of ²⁶Al/¹⁰Be in iron meteorites is constant at 0.70 ± 0.05 (2 σ), independent of pre-atmospheric size (Nagai et al. 1993; Lavielle et al. 1999; Albrecht et al. 2000), the measured ²⁶Al/¹⁰Be ratio of 1.18 ± 0.06 in Pitts

Table 1a. Concentrations of Fe, Ni Co and Si (in wt%) in Horse Creek and Pitts.

	Horse Creek		Pitts	
	This work	Buchwald (1975)	This work	Buchwald (1975)
Fe	91.6	90.4	86	86.5
Ni	5.6	6.3	13.7	12.9
Co	0.39	0.34	0.59	0.52
Si	2.5	2.5	N.D.	–

corresponds to an exposure age of 0.6 (+0.3/–0.2) Myr (Fig. 1) if we assume a simple exposure history. The ³⁶Cl/¹⁰Be production rate ratio in iron meteorites is not constant, but increases from ~3.5 at low shielding to ~6 at high shielding and correlates with the ¹⁰Be concentration (Lavielle et al. 1999). Figure 2 shows that the measured ³⁶Cl/¹⁰Be activity ratio of 11.8 ± 0.3 is best explained by an exposure age of 0.7 ± 0.2 Myr. The radionuclide concentrations in Pitts thus constrain its recent CRE age to 0.7 ± 0.2 Myr and its pre-atmospheric radius to <20 cm.

The concentrations of ³⁶Cl, as well as cosmogenic noble gases, in our Pitts sample are ~40% higher than those reported by Begemann et al. (1970). This systematic difference of ~40% can be explained by a difference in shielding depth of ~7 cm. Unfortunately, detailed information on the relative positions of both samples is lacking (R. Clarke, personal communication). All cosmogenic nuclide data indicate that our sample was irradiated in a less shielded position than the sample measured by Begemann et al. (1970).

From the ³⁸Ar concentration of 0.808×10^{-8} cm³ STP/g and a maximum ³⁸Ar production rate of $0.08\text{--}0.09 \times 10^{-8}$ cm³ STP/g/Myr for small iron meteorites (Begemann et al. 1976; Lavielle et al. 1999), we calculate a minimum ³⁸Ar CRE age of 9–10 Myr. Since the radionuclide data constrain the recent exposure as a small object in space to ~0.7 Myr, our results confirm the conclusions of Begemann et al. (1970) that Pitts has a complex exposure history. Given the difference between the calculated ³⁸Ar age and the ¹⁰Be–²⁶Al–³⁶Cl age, we conclude that more than 90% of the cosmogenic noble gases were produced during the first-stage exposure under higher shielding conditions. Indeed, the high ⁴He/²¹Ne and ⁴He/³⁸Ar ratios (427 and 78) as well as the low ³He/⁴He and ³⁶Ar/³⁸Ar ratios (0.22 and 0.59) in Pitts are all consistent with a scenario in which most of the cosmogenic noble gases were produced under high shielding conditions.

To constrain the duration of the first-stage exposure of Pitts, we first determined the contributions of ⁴He, ²¹Ne, ³⁶Ar, and ³⁸Ar from the first-stage, by subtracting the amounts of these nuclides produced in the second stage from the measured noble gas concentrations (Table 3a). We then estimated the production rates of ⁴He, ²¹Ne, ³⁶Cl, and ³⁸Ar during the first-stage irradiation from the ⁴He/²¹Ne ratio, which is the most sensitive measure of shielding in irons. We corrected the measured ⁴He/²¹Ne ratios of 427 (this work) and

Table 1b. Concentrations of cosmogenic radionuclides (in dpm/kg) in Horse Creek and Pitts. The second columns list the calculated saturation activities and their ratios for the second stage exposure, based on the measured values and second stage CRE ages of 1.0 Myr for Horse Creek and 0.7 Myr for Pitts.

	Horse Creek		Pitts	
	Measured	Calculated	Measured	Calculated
¹⁰ Be	1.73 ± 0.03	4.68 ± 0.09	1.61 ± 0.03	5.36 ± 0.10
²⁶ Al	6.88 ± 0.14	11.0 ± 0.2	1.90 ± 0.09	3.82 ± 0.18
³⁶ Cl	18.6 ± 0.4	20.7 ± 0.4	19.0 ± 0.4	23.7 ± 0.5
⁴¹ Ca	21.4 ± 0.5	21.4 ± 0.5	21.2 ± 1.3	21.4 ± 1.3
²⁶ Al/ ¹⁰ Be	3.98 ± 0.12	2.35 ± 0.07	1.18 ± 0.06	0.71 ± 0.04
³⁶ Cl/ ¹⁰ Be	10.7 ± 0.3	4.42 ± 0.13	11.8 ± 0.3	4.42 ± 0.13
⁴¹ Ca/ ³⁶ Cl	1.15 ± 0.04	1.04 ± 0.04	1.12 ± 0.07	0.90 ± 0.06

Table 2. Measured and cosmogenic noble gas concentrations (in 10⁻⁸ cm³ STP/g) in the Horse Creek (488 mg) and Pitts (79 mg) irons. The last column lists the average cosmogenic concentrations and ratios of the noble gas analyses in two aliquots of Pitts by Begemann et al. (1970). All errors correspond to 2σ uncertainties.

	Horse Creek (this work)		Pitts (this work)		Pitts
	Measured	Cosmogenic	Measured	Cosmogenic	Cosmogenic
³ He	3.24 ± 0.15	3.24 ± 0.15	13.8 ± 0.5	13.8 ± 0.5	10.0
⁴ He	17.9 ± 0.8	17.9 ± 0.8	63.1 ± 2.4	163.1 ± 2.4	46.0
²⁰ Ne	0.088 ± 0.004	0.088 ± 0.004	0.159 ± 0.007	0.133 ± 0.007	–
²¹ Ne	0.091 ± 0.004	0.091 ± 0.004	0.148 ± 0.006	0.148 ± 0.006	0.100
²² Ne	0.109 ± 0.005	0.109 ± 0.005	0.159 ± 0.007	0.156 ± 0.006	–
³⁶ Ar	0.198 ± 0.007	0.183 ± 0.007	0.529 ± 0.009	0.481 ± 0.008	0.345
³⁸ Ar	0.327 ± 0.011	0.324 ± 0.011	0.817 ± 0.012	0.808 ± 0.012	0.590
⁴⁰ Ar	4.59 ± 0.16	–	15.0 ± 0.4	–	–
³ He/ ⁴ He	0.180 ± 0.002	0.180 ± 0.002	0.219 ± 0.002	0.219 ± 0.002	0.217
³ He/ ³⁸ Ar	10.0 ± 0.6	10.0 ± 0.6	16.9 ± 0.7	17.1 ± 0.7	16.9
⁴ He/ ³⁸ Ar	54.7 ± 3.1	55.3 ± 3.1	77.2 ± 3.2	78.1 ± 3.2	78.0
⁴ He/ ²¹ Ne	198 ± 12	198 ± 12	427 ± 25	427 ± 25	462 ± 14
³⁶ Ar/ ³⁸ Ar	0.606 ± 0.003	0.565 ± 0.003	0.648 ± 0.004	0.595 ± 0.005	0.585

462 (Begemann et al. 1970) in the two Pitts samples for contributions of ⁴He and ²¹Ne produced in the second stage. These corrections yield ⁴He/²¹Ne ratios of 442 ± 24 and 479 ± 25 for the first-stage exposure of Pitts (Table 3a). These ⁴He/²¹Ne ratios are somewhat higher than the range (200–450) generally observed in iron meteorites (Voshage and Feldman 1979; Voshage et al. 1983; Lavielle et al. 1999), but overlap with those observed in very large irons, such as Canyon Diablo (Heymann et al. 1966) and Odessa (Herzog et al. 1976), and in metal phases of the large Brenham pallasite, which has a minimum pre-atmospheric radius of ~3 m (Honda et al. 2002). The high ⁴He/²¹Ne ratios in Pitts thus suggest that the first-stage irradiation occurred in a very large object. Based on Equation 16 in Honda et al. (2002), the ⁴He/²¹Ne ratios of 442 ± 24 and 479 ± 25 for the first-stage irradiation of Pitts correspond to irradiation depths of 490–600 g/cm² or 63–77 cm (assuming a density of 7.8 g/cm³).

To estimate the production rates of ⁴He, ²¹Ne, ³⁸Ar and ³⁶Cl during the firststage irradiation of Pitts, we assumed similar (near-2π) shielding conditions as in the Brenham pallasite. Based on experimental data for a 156 ± 8 Myr CRE age of Brenham and empirical formulas (Honda et al. 2002), the following correlations between the production rates, P,

and the ⁴He/²¹Ne ratios in metal samples of the Brenham pallasite were derived (Fig. 3):

$$\log[P(^4\text{He})] = 17.34 - 6.168 \cdot \log[^4\text{He}/^{21}\text{Ne}], \quad (1)$$

$$\log[P(^{21}\text{Ne})] = 16.78 - 6.953 \cdot \log[^4\text{He}/^{21}\text{Ne}], \quad (2)$$

$$\log[P(^{38}\text{Ar})] = 16.55 - 6.575 \cdot \log[^4\text{He}/^{21}\text{Ne}], \quad (3)$$

and

$$\log[P(^{36}\text{Cl})] = 16.56 - 6.424 \cdot \log[^4\text{He}/^{21}\text{Ne}]. \quad (4)$$

The production rates of ⁴He, ²¹Ne, ³⁸Ar are expressed in 10⁻¹⁰ cm³ STP/g per Myr and the production rate of ³⁶Cl is expressed in atoms/min/kg. The noble gas production rates for the first-stage irradiation of Pitts can now be derived from Equations 1–3 and the inferred ⁴He/²¹Ne ratios of 442 ± 24 and 479 ± 25 for the two Pitts samples. The first-stage CRE age of Pitts is calculated from the first-stage ⁴He, ²¹Ne and ³⁸Ar contributions and the corresponding production rates (Table 3a). In addition, we calculated the first-stage CRE age using the ³⁶Cl-³⁶Ar method, which is shielding independent (Schaeffer and Heymann 1965). The ³⁶Cl-³⁶Ar age, T₃₆, is calculated using the following expression (Lavielle et al. 1999):

$$T_{36} = 427 \cdot [^{36}\text{Ar}]/P(^{36}\text{Cl}), \quad (5)$$

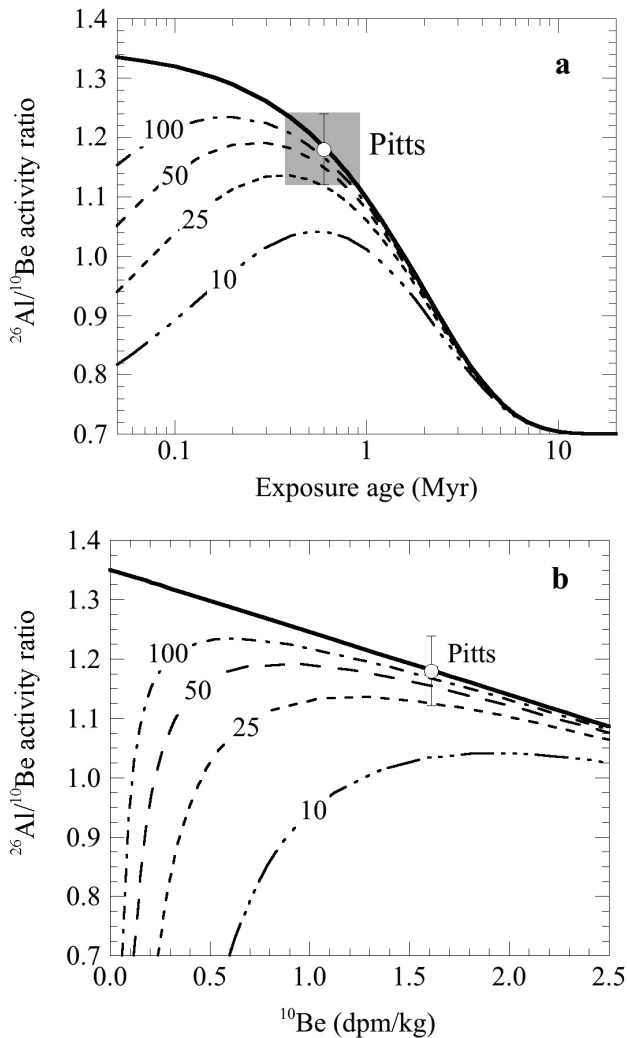


Fig. 1. Comparison of the measured $^{26}\text{Al}/^{10}\text{Be}$ ratio of 1.18 ± 0.06 in Pitts with calculated ratios for simple and complex exposure histories. The curves in Fig. 1 show the expected relation between the $^{26}\text{Al}/^{10}\text{Be}$ ratio and either the exposure age (a) or the ^{10}Be concentration (b) as a function of exposure age. The solid lines assume a simple exposure history with $P(^{10}\text{Be}) = 6$ dpm/kg and a $^{26}\text{Al}/^{10}\text{Be}$ production rate ratio of 0.7, while the dashed curves are based on complex exposure histories with first-stage ^{10}Be and ^{26}Al production rates that were 10, 25, 50, and 100 times lower than in the recent exposure. The measured $^{26}\text{Al}/^{10}\text{Be}$ ratio and ^{10}Be concentration in Pitts can either be explained by a simple exposure age of $0.6 (+0.3/-0.2)$ Myr or a complex exposure history with first-stage production rates at least a factor of 25 lower than in the most recent exposure.

in which the ^{36}Ar concentration, $[^{36}\text{Ar}]$, is expressed in 10^{-8} cm^3 STP/g and the ^{36}Cl production rate, $P(^{36}\text{Cl})$, in atoms/min/kg.

The four ages are internally consistent and yield average first-stage CRE ages of 546 ± 19 Myr for the sample studied in this work and 659 ± 13 Myr for the sample analyzed by Begemann et al. (1970). The quoted errors only reflect the standard deviation of the four ages, whereas the uncertainty in the first-stage $^4\text{He}/^{21}\text{Ne}$ ratios yields an uncertainty of $\sim 30\%$ in the absolute production rates. We thus adopt an average first-

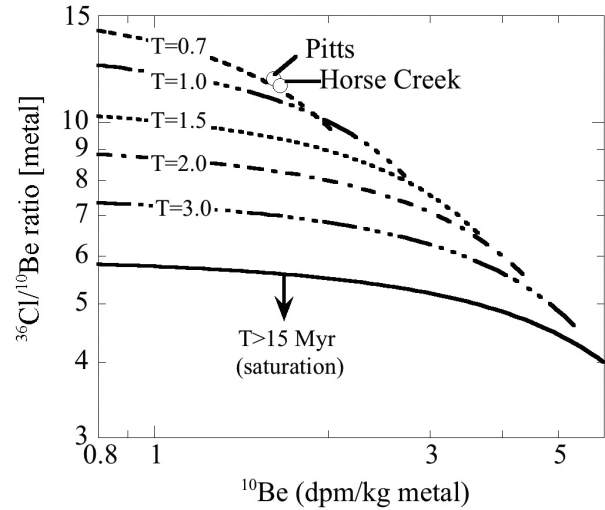


Fig. 2. Constraints on the CRE age of Pitts from measured $^{36}\text{Cl}/^{10}\text{Be}$ activity ratios. Based on the empirical correlation of $^{36}\text{Cl}/^{10}\text{Be}$ versus ^{10}Be in iron meteorite falls (solid line; Lavielle et al. 1999), the measured $^{36}\text{Cl}/^{10}\text{Be}$ ratio of 11.8 ± 0.3 in Pitts corresponds to a CRE age of ~ 0.7 Myr. Similarly, if we correct the measured ^{10}Be concentration in Horse Creek for a small ($\sim 5\%$) contribution of ^{10}Be from Si, the corrected $^{36}\text{Cl}/^{10}\text{Be}$ ratio also corresponds to a CRE age of ~ 0.7 Myr.

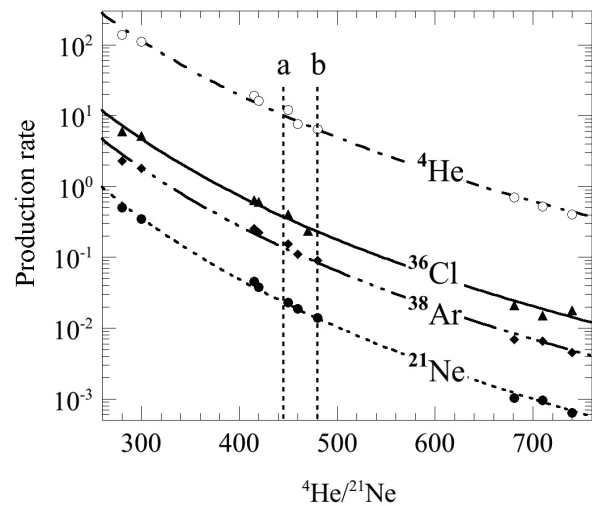


Fig. 3. Production rates of ^4He , ^{21}Ne and ^{38}Ar (in 10^{-10} cm^3 STP/g per Myr) and of ^{36}Cl (in atoms/min per kg) as a function of the $^4\text{He}/^{21}\text{Ne}$ ratio in metal phases of the 156 Myr CRE age of Brenham pallasite (Honda et al. 2002). Since the measured $^4\text{He}/^{21}\text{Ne}$ ratios show some scatter due to the very low ^{21}Ne concentrations at high shielding, we used model-derived $^4\text{He}/^{21}\text{Ne}$ ratios based on ^3He concentrations (Honda et al. 2002). Production rates corresponding to the inferred $^4\text{He}/^{21}\text{Ne}$ ratios of 442 and 479 for the first-stage irradiation of the two Pitts samples are shown by the two dashed vertical lines. The powerlaw fits shown in the figure correspond to Equations 1–4 in the text.

stage CRE age of $600 (+190/-150)$ Myr for Pitts, which is in the range of typical CRE ages of most other iron meteorites.

The estimated ^{36}Cl production rates of $0.3\text{--}0.5$ atom/min/kg for the first-stage irradiation of Pitts are almost two orders of magnitude lower than is typical ($20\text{--}25$ atom/min/kg) for

Table 3a. First-stage exposure age of Pitts, based on calculated noble gas contributions from the first stage irradiation (in 10^{-8} cm³ STP/g). These contributions were derived from the measured concentrations of Table 2 by subtracting the amounts produced during the recent exposure of ~ 0.7 Myr. Production rates (in 10^{-10} cm³ STP/g per Myr) of ⁴He (P₄), ²¹Ne (P₂₁), ³⁸Ar (P₃₈) as well as the production rate (in atom/min/kg) of ³⁶Cl (P₃₆) at the first stage, were calculated using empirical formulas of Honda et al. (2002) and the first-stage ⁴He/²¹Ne ratio from column 6.

Sample	⁴ He	²¹ Ne	³⁶ Ar	³⁸ Ar	⁴ He/ ²¹ Ne	P ₄	P ₂₁	P ₃₈	P ₃₆	T ₄	T ₂₁	T ₃₈	T ₃₆	T _{avg}
Pitts-a)	59.9	0.135	0.461	0.755	442 ± 24	10.5	0.0243	0.143	0.368	568	556	527	535	546 ± 19
Pitts-b)	42.7	0.088	0.324	0.550	479 ± 25	6.4	0.0139	0.084	0.220	676	651	662	648	659 ± 13

a) This work, b) noble gas data from Begemann et al. (1970).

Table 3b. First-stage exposure age (T₃₆) of Horse Creek, based on the ³⁶Cl-³⁶Ar method and ³⁶Ar concentrations from the first stage exposure. These first-stage concentrations (1) were derived from measured (m) ³⁶Ar and ³⁸Ar concentrations, corrected for contributions from the second-stage exposure (2). The ³⁶Cl production rate, P(³⁶Cl), during the first-stage exposure of Horse Creek was derived from Equation 6.

Sample	³⁸ Ar (10 ⁻⁸ cm ³ STP/g)			³⁶ Ar (10 ⁻⁸ cm ³ STP/g)			³⁶ Ar/ ³⁸ Ar	P(³⁶ Cl)	T ₃₆
	(m)	(1)	(2)	Meas.	(1)	(2)	(1)	dpm/kg	Myr
Horse	0.324	0.249	0.075	0.183	0.150	0.033	0.602	0.64	100
Creek	±0.011	±0.008	±0.007	±0.007	±0.006	±0.003	±0.003	+0.24/-0.18	+40/-30

small iron meteorites (Nishiizumi 1995). These low first-stage production rates are consistent with our earlier conclusion derived from the ²⁶Al/¹⁰Be ratio. Given the second-stage exposure of ~ 0.7 Myr, these low first-stage production rates imply that the contributions of ¹⁰Be, ²⁶Al, and ³⁶Cl from the first-stage irradiation are $<3.5\%$, $<1.5\%$ and $<0.5\%$ of the measured ¹⁰Be, ²⁶Al, and ³⁶Cl concentrations, respectively. Given the experimental uncertainties of 2–5%, the cosmogenic radionuclide concentrations thus show no detectable evidence of the first-stage exposure history. This implies that based on the cosmogenic nuclide records alone we can not constrain whether the first-stage irradiation of Pitts occurred early in the meteoroid's history on the IAB iron meteorite parent body or immediately prior to the recent collision that excavated Pitts from its parent meteoroid ~ 0.7 Myr ago. Although future measurements of long-lived ⁵³Mn ($t_{1/2} = 3.7$ Myr) may shed more light on this issue, we will argue below that irradiation on a large precursor meteoroid is the most plausible scenario in the light of current meteorite delivery models (Gladman et al. 1997; Bottke et al. 2000).

Horse Creek

The concentrations of ³⁶Cl and ⁴¹Ca are similar to saturation values of small irons, indicating that Horse Creek had a small pre-atmospheric mass. The ⁴¹Ca concentration of 21.4 ± 0.5 dpm/kg implies a terrestrial age <20 kyr, making corrections for radioactive decay of ¹⁰Be and ²⁶Al during terrestrial residence negligible. Due to the presence of 2.5 wt% Si in the metal, the ¹⁰Be, ²⁶Al and Ne isotope results are interpreted using model calculations. Based on model calculations (e.g., Masarik and Reedy 1994), the elemental production rate of ²⁶Al and Ne isotopes from Si is, depending

on shielding conditions, 40–200 times higher than that from Fe. The presence of 2.5 wt% Si thus significantly increases the ²⁶Al and Ne isotope production in this iron meteorite, by a factor of 2–6, whereas it increases the ¹⁰Be production rate by only 4–6%. Figure 4 shows production rates of ²⁶Al (a) and ¹⁰Be (b) in iron meteorites containing 91 wt% Fe, 5.6 wt% Ni, 0.4 wt% Co, 2.5 wt% Si, and 0.5 wt% P, calculated using LCS (Masarik and Reedy 1994). The measured ¹⁰Be and ²⁶Al concentrations of 1.73 and 6.9 dpm/kg in Horse Creek constrain the CRE age to 0.8–1.2 Myr, while the ³⁶Cl/¹⁰Be ratio of ~ 11 constrains the CRE age to <1 Myr (Fig. 2). Figure 5 shows that the best agreement between the measured ²⁶Al and ¹⁰Be concentrations in Horse Creek and the calculated production rates is found for a CRE of 0.9–1.0 Myr, corresponding to irradiation at a depth of 5–10 cm in an object of 15–25 cm in radius.

The ³⁸Ar concentration in Horse Creek requires a minimum CRE age of 4–5 Myr, significantly higher than the radionuclide exposure age of ~ 1.0 Myr. This implies that Horse Creek also experienced a complex exposure history and that 75–80% of the ³⁸Ar (and other cosmogenic noble gases) was formed in a previous exposure under higher shielding conditions. The cosmogenic noble gas results in Horse Creek cannot simply be compared with those of other iron meteorites because of the high abundance of Si in Horse Creek. The presence of Si in iron meteorites affects the production rates of He and Ne isotopes, but not those of Ar isotopes. The common noble gas shielding indicators, such as ³He/⁴He, ⁴He/²¹Ne, ⁴He/³⁸Ar, and ²¹Ne/³⁸Ar are not reliable for the Horse Creek iron, leaving the ³⁶Ar/³⁸Ar ratio as the only useful shielding indicator. Furthermore, the measured ³He/³⁸Ar ratio in Horse Creek is $\sim 40\%$ lower than the average value of 16.7 ± 0.5 in iron meteorites (Voshage and Feldman 1979; Honda et al. 2002). Although about 25% of the iron

meteorites studied by Voshage and Feldmann (1979) show ^3He deficiencies, these deficiencies are generally <15% and are attributed to loss of tritium (^3H) during irradiation (Schultz 1967). The large deficiency (~40%) of ^3He in Horse Creek suggests that ^3He was lost by a different mechanism, possibly during the recent break-up event, and was probably associated with loss of cosmogenic ^4He .

The cosmogenic $^{36}\text{Ar}/^{38}\text{Ar}$ ratio in iron meteorites with $^4\text{He}/^{21}\text{Ne}$ ratios of 200–450 ranges from 0.60–0.66 and shows a negative correlation with the $^4\text{He}/^{21}\text{Ne}$ ratio (Voshage and Feldmann 1979). The $^{36}\text{Ar}/^{38}\text{Ar}$ ratio of 0.565 ± 0.003 in Horse Creek is one of the lowest values reported for an iron meteorite. Since 83% of the cosmogenic ^{36}Ar in iron meteorites is produced via decay of ^{36}Cl and the second-stage exposure of Horse Creek is only ~1 Myr, the ^{36}Cl - ^{36}Ar pair is not in secular equilibrium (e.g., Begemann et al. 1970). If we assume a $^{36}\text{Ar}/^{38}\text{Ar}$ ratio of 0.65 ± 0.01 for small iron meteorites with long exposure ages (Lavielle et al. 1999) and a second-stage exposure of 1 Myr for Horse Creek, then the observed $^{36}\text{Ar}/^{38}\text{Ar}$ ratio of 0.565 ± 0.003 requires a $^{36}\text{Ar}/^{38}\text{Ar}$ ratio of 0.602 ± 0.003 for the first-stage irradiation of Horse Creek. This low $^{36}\text{Ar}/^{38}\text{Ar}$ ratio clearly indicates high shielding conditions for the first-stage irradiation of Horse Creek, corresponding to a $^4\text{He}/^{21}\text{Ne}$ ratio of ~450, a $^4\text{He}/^{38}\text{Ar}$ ratio of ~73 and a $^{21}\text{Ne}/^{38}\text{Ar}$ ratio of ~0.17 for regular iron meteorites with the same shielding conditions (Voshage and Feldmann 1979; Lavielle et al. 1999). The low $^4\text{He}/^{38}\text{Ar}$ ratio of ~55 in Horse Creek thus suggests that ~25% of the cosmogenic ^4He was lost (most likely during the recent break-up event), while the high $^{21}\text{Ne}/^{38}\text{Ar}$ ratio of ~0.28 indicates that ~40% of the total ^{21}Ne in Horse Creek was produced from Si. These two effects also explain the low $^4\text{He}/^{21}\text{Ne}$ ratio of ~200 found in Horse Creek.

Typical $^{22}\text{Ne}/^{21}\text{Ne}$ ratios in iron meteorites are 1.04–1.08 (Lavielle et al. 1999). The high $^{22}\text{Ne}/^{21}\text{Ne}$ ratio of ~1.20 in Horse Creek seems to be due to a combination of the high Si content and high shielding conditions of the first-stage irradiation. Calculations of ^{21}Ne and ^{22}Ne production rates (Masarik et al. 2001) show that the addition of 2.5 wt% Si to metal increases to values ranging from 1.10 at low shielding to >1.25 at high shielding (Fig. 6). For the second-stage irradiation at 5–10 cm depth in a 15–25 cm radius object, the calculated $^{22}\text{Ne}/^{21}\text{Ne}$ ratio is 1.15. The calculations also show that, at high shielding conditions, the production rate of ^{21}Ne from Si is a factor of 100–150 times higher than from FeNi, which implies that during the first stage irradiation 70–80% of the cosmogenic Ne in Horse Creek was produced from Si, and only 20–30% from FeNi. Since 20–25% of the cosmogenic noble gases was produced during the second stage irradiation, the $^{22}\text{Ne}/^{21}\text{Ne}$ ratio in the first stage was calculated to be 1.21–1.22. The high $^{22}\text{Ne}/^{21}\text{Ne}$ ratio is consistent with irradiation under high shielding, i.e., at a depth of >20 cm in an object with a radius >40 cm (Fig. 6). The measurements of cosmogenic nuclides in meteorites with unusual compositions, such as Horse Creek, provide critical tests of various model

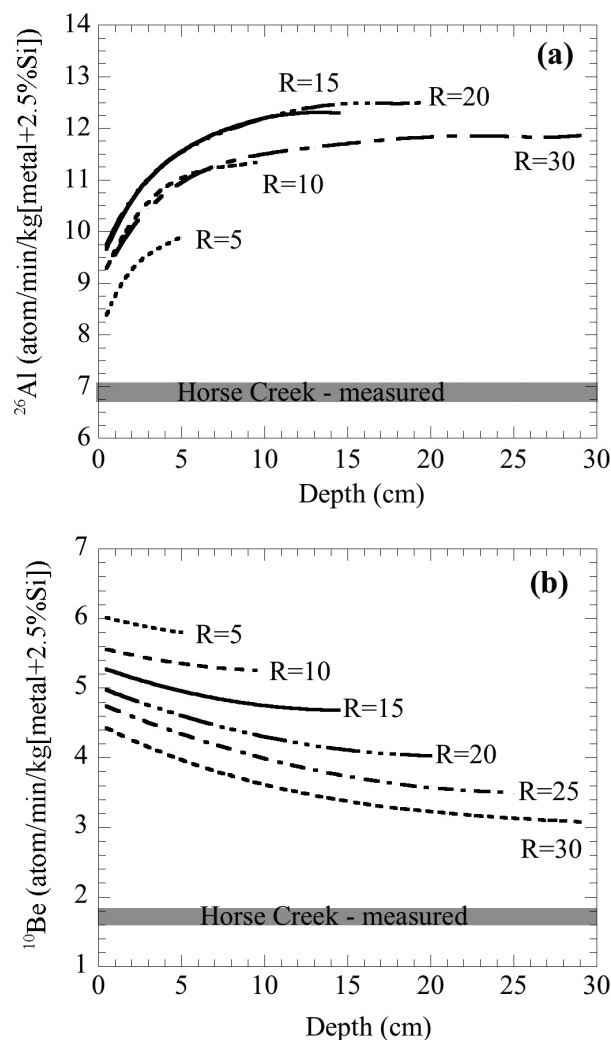


Fig. 4. Production rates of ^{26}Al (a) and ^{10}Be (b) versus depth in iron meteorites with radii of 5–30 cm and 2.5 wt% Si. Production rates were calculated using the LCS model (Masarik and Reedy 1994). The measured concentrations of ^{26}Al and ^{10}Be in Horse Creek are indicated by grey bands.

calculations. The high $^{22}\text{Ne}/^{21}\text{Ne}$ ratio in Horse Creek is in good agreement with the model calculation by Masarik et al. (2001), whereas the model calculations by Leya et al. (2000, 2001) predict a relatively constant $^{22}\text{Ne}/^{21}\text{Ne}$ ratio from Si and a steep increase in the $^{22}\text{Ne}/^{21}\text{Ne}$ ratio from Fe, which cannot be reconciled with the ratio of 1.20 found in Horse Creek.

To calculate the duration of the first-stage exposure of Horse Creek, we first corrected the measured ^{36}Ar and ^{38}Ar concentrations for contributions produced during the second stage exposure of ~1 Myr as a small object (Table 3b), and then estimated the first-stage production rate of ^{36}Cl (and ^{36}Ar) from the $^{36}\text{Ar}/^{38}\text{Ar}$ ratio. Figure 7 shows that $P(^{36}\text{Cl})$ is strongly correlated with the $^{36}\text{Ar}/^{38}\text{Ar}$ ratio in metal phases of the Brenham meteorite (Honda et al. 2002), yielding the following equation (which is only valid for very large objects with long

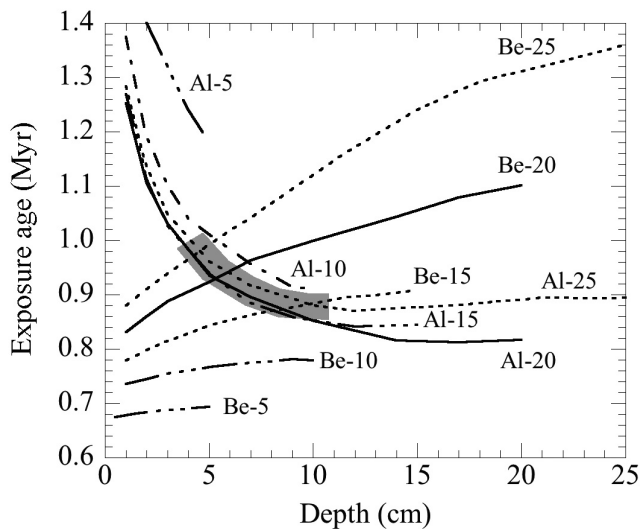


Fig. 5. Cosmic-ray exposure ages derived from measured concentrations of ^{10}Be and ^{26}Al in Horse Creek and calculated production rates of ^{10}Be and ^{26}Al in irons with radii of 5–25 cm and 2.5 wt% Si (see Fig. 4). The shaded area represents the exposure conditions for which the measured ^{10}Be and ^{26}Al concentrations and model calculations yield a consistent scenario, i.e., irradiation at a depth of 5–10 cm in objects with radii of 15–25 cm. These conditions constrain the recent CRE age of Horse Creek to 0.9–1.0 Myr.

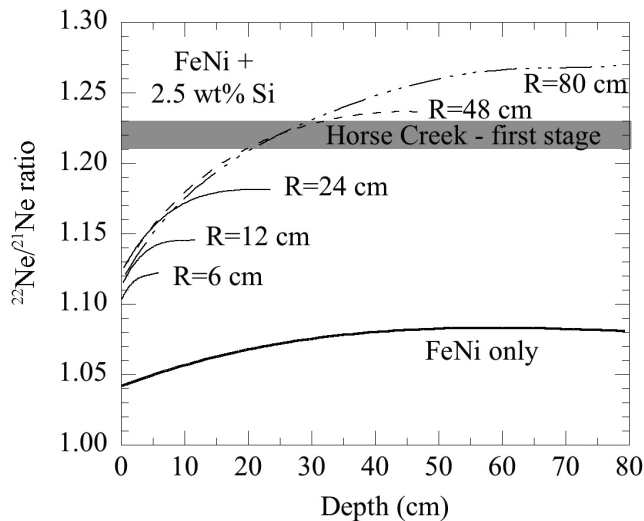


Fig. 6. Calculated $^{22}\text{Ne}/^{21}\text{Ne}$ ratios in iron meteorites with radii of 6–80 cm, using the model calculation (Masarik et al. 2001). We increased the calculated $^{22}\text{Ne}/^{21}\text{Ne}$ ratios from FeNi only (solid line) by $\sim 20\%$ to improve agreement with measured ratios of 1.04–1.08 in regular iron meteorites (Lavielle et al. 1999). The dashed lines represent calculated $^{22}\text{Ne}/^{21}\text{Ne}$ ratios in iron meteorites with radii of 6–80 cm containing 2.5 wt% Si.

CRE ages and $^{36}\text{Ar}/^{38}\text{Ar}$ ratios in the range of 0.58–0.63):

$$\log[P(^{36}\text{Cl})] = 46.6 * [^{36}\text{Ar}/^{38}\text{Ar}] - 28.25, \quad (6)$$

Based on Equation 6, and the first-stage $^{36}\text{Ar}/^{38}\text{Ar}$ ratio of 0.602 ± 0.003 we estimate a ^{36}Cl production of $0.64 (+0.24/-0.18)$ atoms/min/kg for the first-stage irradiation of Horse Creek

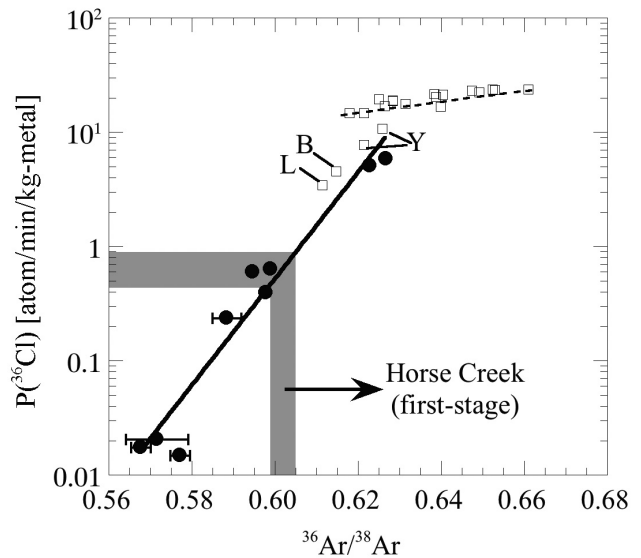


Fig. 7. Variation of the ^{36}Cl production rate, $P(^{36}\text{Cl})$, in iron meteorites (open symbols; Lavielle et al. 1999) and metal phases of the Brenham pallasite (solid symbols; Honda et al. 2002) as a function of the $^{36}\text{Ar}/^{38}\text{Ar}$ ratio. The solid line represents the correlation (Equation 6) between $P(^{36}\text{Cl})$ and the $^{36}\text{Ar}/^{38}\text{Ar}$ ratio in metal phases of the large Brenham pallasite and three large iron meteorites (B = Bendego, L = Lombard, Y = Yanhuitan). For comparison, the dashed line corresponds to a similar correlation for irons less than ~ 1 m in diameter (open symbols). Based on a first-stage $^{36}\text{Ar}/^{38}\text{Ar}$ ratio of 0.602 ± 0.003 , we estimate $P(^{36}\text{Cl}) = 0.64 (+0.24/-0.18)$ atom/min/kg for the first-stage irradiation of Horse Creek.

(Fig. 7). This production rate yields a first-stage ^{36}Cl - ^{36}Ar exposure age of 100 (+40/–30) Myr for Horse Creek (Table 3b). This first-stage CRE age is on the low end of the typical range for iron meteorites, and on the high end of the range of 20–120 Myr for aubrites (Lorenzetti et al. 2003). Based on the low ^{36}Cl production, we estimate that the first-stage irradiation of Horse Creek took place at a depth of ~ 60 cm in an object with a radius > 1 m. Due to the low production rates during the first stage, contributions of ^{10}Be from the first-stage irradiation of Horse Creek are $< 5\%$ of the measured ^{10}Be concentration, while relative contributions of ^{26}Al and ^{36}Cl are even a factor of 2–10 lower. Given the uncertainties in the measured concentrations and in the calculated production rates, we are unable to detect these small contributions.

Implications for Meteorite Delivery Models

Horse Creek and Pitts are the first two irons for which the cosmogenic nuclide records provide unambiguous evidence for a complex exposure history with a short second stage, which is well constrained by the undersaturated concentrations of ^{26}Al and ^{10}Be . Complex exposure histories have previously been proposed for several other iron meteorites, such as Canyon Diablo, Odessa and Sikhote Alin, but the second-stage exposure ages of these large irons were much longer, in the range of 75–200 Myr. The unique

exposure histories of Horse Creek and Pitts thus provide new insight into the delivery mechanism of iron meteorites from the asteroid belt to Earth.

Most significantly, the second-stage exposure ages of 0.7–1 Myr for Pitts and Horse Creek are very similar to the expected delivery times of meteoroids injected into one of the orbital resonances (Gladman et al. 1997; Morbidelli and Gladman 1998). We thus conclude that the recent breakup events of Horse Creek and Pitts occurred when their precursor objects were either near one of the orbital resonances, thus injecting collisional fragments into these chaotic escape zones, or already in Earth-approaching or Earth-crossing orbits. Although both scenarios provide a quick delivery route of meteoroids to Earth, we cannot distinguish between the two, as they involve chaotic processes. If the precursor objects were already in Earth-crossing orbits, they must have been injected into these orbits within the last few Myr, since the dynamical lifetimes of objects in eccentric orbits with semimajor axis in the main belt are short (Gladman et al. 1997). In either scenario, the first-stage irradiations of Horse Creek (~100 Myr) and Pitts (~600 Myr) predominantly occurred while these irons traveled as large objects in the main asteroid belt and thus represent the long “storage times” of iron meteoroids in the asteroid belt. These long storage times of irons are consistent with the slow Yarkovsky-driven orbital drift rates ($<5 \times 10^{-4}$ AU/Myr) of iron meteoroids from the main asteroid belt to one of the chaotic escape zones (Farinella et al. 1998; Hartmann et al. 1999).

It is plausible that most iron meteorites follow this two-step delivery mechanism, but the cosmogenic nuclide record can only distinguish between the “slow orbital drift in the asteroid belt” and the “quick delivery to Earth” if recent collisions in (or near) these chaotic escape zones broke up precursor objects before delivering small fragments to Earth. Based on material properties (crushing strength) of iron meteorites and average collisional probability and meteoroid size distribution in the main asteroid belt, Farinella et al. (1998) calculated a collisional lifetime of 1.4 Gyr for iron meteoroids with a radius of 1 m. Since collisional disruption events are relatively rare for iron meteorites, we expect that most irons traveled from the asteroid belt to Earth without any secondary break-up events, while a few show secondary break-up events during the course of their long CRE history. This is consistent with the general CRE histories of iron meteorites (Voshage et al. 1983).

Given the long collisional lifetime of meter-sized irons, the discovery of two iron meteorites (out of a total of 50–100 that have been studied) with very recent collisional disruption events seems statistically unlikely. A possible explanation could be that the parent objects of Horse Creek and/or Pitts were already in Earth-crossing orbits at the time of the recent break-up event. According to model calculations of Bottke et al. (1996), the frequency of catastrophic disruption increases by a factor of ~5 when the orbital eccentricity (e) of

meteoroids in the main belt increases from $e < 0.1$ (near-circular) to $e \sim 0.6$ (Earth-crossing), mainly as a result of higher impact velocities. This effect could reduce the collisional lifetime to a few hundred Myr, still much longer than the orbital lifetime of a few Myr, but short enough that a small percentage of the irons in Earth-crossing orbits experiences a collisional disruption before colliding with Earth. An alternative explanation is that Horse Creek and Pitts represent collisional debris from relatively small impacts on km-sized parent bodies, as we will discuss below.

Although the timing of the recent breakup events of Horse Creek and Pitts is well constrained by the radionuclide records, and the duration of the first-stage exposure is reasonably well constrained by the noble gas records, the size of the precursor objects is less well constrained. The cosmogenic noble gas ratios indicate that the first-stage irradiation occurred under high shielding, but they cannot distinguish between irradiation in an object several meters in radius (a large meteoroid) or a few km in radius (a small asteroid). Given the short second-stage exposure ages of Pitts and Horse Creek, we cannot exclude the possibility that these two irons were ejected during small impacts on km-sized near-Earth objects (NEO). Based on the intrinsic collisional probability and size frequency distribution of the meteoroid population (Farinella et al. 1998), we estimate that a km-sized asteroid is hit once in 1 Myr by an object of 4–5 m in radius, which is large enough to excavate fragments from less than 1 m deep (Melosh 1984). Ejection of these fragments from NEOs would provide a quick delivery route to Earth, consistent with the observed second-stage exposure ages of Horse Creek and Pitts.

Horse Creek is an ungrouped iron, which is presumably related to the aubrites, as suggested by its trace element composition (Casanova et al. 1993). Therefore, Horse Creek is most likely linked to the E-type asteroids, which are the closest match (in terms of reflectance spectra) to aubrites. Considering its short second-stage exposure age, a plausible source object for Horse Creek is the Earth-crossing E-type asteroid 3103 Eger, which was previously proposed as the parent body of many aubrites and is believed to be linked to the Hungaria region at the innermost edge (1.9 AU) of the asteroid belt (Gaffey et al. 1992). However, unlike the aubrites, which have CRE ages of 20–120 Myr (Lorenzetti et al. 2003), mostly as small to medium sized objects in space (Welten et al. 2004), Horse Creek was only exposed as a small object in space for ~1 Myr and is thus more likely to represent collisional debris from a NEO than the aubrites themselves.

The most likely source for most iron meteorites are the M-type asteroids, which show relative featureless reflectance spectra, consistent with the presence of FeNi metal. However, not all M-type asteroids are related to iron meteorites, as recent studies have suggested that some M-type objects may have chondritic compositions (cf. Rivkin et al. 2000; Burbine et al. 2002; Magri et al. 2007). Tedesco and Gradie (1987)

found two M-type objects (3554 Amun and 1986 DA) in the NEO population and concluded that iron meteorites derived from these NEOs should have low CRE ages. Radar observations have confirmed a metallic composition for asteroid 1986 DA (Ostro et al. 1991), while the composition of 3554 Amun is still uncertain. Since impacts on a small (2 km) NEO would provide a quick delivery of fragments to Earth, asteroid 1986 DA seems a plausible source for the Pitts iron, which has a second-stage exposure of ~ 0.7 Myr. Based on the short dynamical lifetime of asteroid 1986 DA, this NEO most likely represents a collisional fragment from a larger M-type asteroid in the main belt. Interestingly, the semi-major axis of 1986 DA (2.81 AU) is very close to the 5:2 mean motion resonance (at ~ 2.82 AU) with Jupiter. This may suggest that the ultimate parent body from which 1986 DA (and possibly Pitts) originated, was close to the 5:2 resonance. Of the approximately 50 M-type asteroids (with diameters between 30 and 250 km) in the main belt, 14 are within 0.1 AU from the 5:2 resonance, including two of the largest M-type asteroids with metallic compositions (Magri et al. 2007), 16 Psyche (D \sim 250 km) and 216 Kleopatra (217 \times 94 \times 81 km). If 1986 DA is the immediate parent object of the Pitts IAB iron, then it seems plausible that the main parent body of the IAB irons is located near the 5:2 resonance. Although the 5:2 resonance is not very efficient in delivering meteorites to Earth (Morbidelli and Gladman 1998), and thus is not considered a major source region for chondrites, it could be a viable source region of IAB irons, which only represent $\sim 0.5\%$ of all meteorite falls (Grady 2000). In fact, a source of IAB irons near the 5:2 resonance is consistent with conclusions of Voshage et al. (1983), who argued that the lack of clusters in the CRE age distribution of IAB irons indicates that impacts on the IAB parent body are less efficient in delivering material to Earth than impacts on the IIIAB or IVA iron meteorite parent bodies.

Although the proposed links between the Pitts IAB iron and asteroid 1986 DA (or any M-type asteroid), and between the Horse Creek iron and asteroid 3103 Eger are still speculative, these two irons are the most likely candidates among iron meteorites to be linked to NEOs, based on their short irradiation times as small objects. However, since detailed exposure age studies using multiple cosmogenic radionuclides have only been carried out for a limited number of iron meteorites, it cannot be excluded that more irons with short delivery times will be found.

SUMMARY

The cosmogenic nuclide concentrations in two genetically unrelated iron meteorites, Horse Creek (ungrouped) and Pitts (IAB), provide unambiguous evidence for complex exposure histories. The noble gas records reveal a first-stage exposure of 100–600 Myr under high shielding conditions, while the cosmogenic radionuclides indicate a

recent irradiation of ~ 1 Myr in objects with radii of 15–25 cm. The long first-stage exposure ages are consistent with typical CRE ages of iron meteorites, and most likely represent the long Yarkovsky orbital drift times from their parent bodies in the asteroid belt to one of the secular or mean motion resonance zones (Bottke et al. 2000), while the recent exposure ages of ~ 1 Myr are similar to the expected delivery times (to Earth) of collisional fragments “injected” into one of these chaotic resonances (Gladman et al. 1997). The time scales of the two processes involved in the delivery of Horse Creek and Pitts from the asteroid belt to Earth are consistent with current meteorite delivery models (Gladman et al. 1997; Bottke et al. 2000).

The cosmogenic nuclide data only constrain the size of the precursor objects of Horse Creek and Pitts to a minimum radius of a few meters, but do not provide an upper limit. Therefore, it is possible that Horse Creek and Pitts were ejected ~ 1 Myr ago from km-sized near-Earth objects, such as E-type asteroid 3103 Eger and M-type asteroid 1986 DA, respectively. Although still speculative, these would be the first links between iron meteorites and specific asteroids.

We used the unusual composition of Horse Creek to evaluate the effect of Si on the production rates of ^{26}Al , ^{21}Ne and ^{22}Ne in metallic FeNi. Assuming a recent CRE age of ~ 1 Myr, the measured concentration of ^{26}Al in Horse Creek is in good agreement with model calculations (Masarik and Reedy 1994; Leya et al. 2000, 2001). Although the high $^{22}\text{Ne}/^{21}\text{Ne}$ ratio observed in Horse Creek agrees much better with calculations for the production of Ne from Si using the model of Masarik et al. (2001) than with those using the model of Leya et al. (2000, 2001), experimental results show that more reliable cross section data are needed for improvement in the calculation of ^{21}Ne and ^{22}Ne production rates from Fe.

Acknowledgments—We thank R. Clarke and T. McCoy of the Smithsonian Institution for providing samples of the Pitts and Horse Creek meteorites. We also thank F. Begemann and W. F. Bottke for valuable discussions and O. Eugster, R. Wieler and A. J. T. Jull for constructive reviews. This work was supported by NASA grants NAG5-4992 and NAG5-12846, an LLNL-CAMS grant, and was performed under the auspices of the U.S. DOE by LLNL under contract W-7405-ENG-48.

Editorial Handling—Dr. A. J. Timothy Jull

REFERENCES

- Albrecht A., Schnabel S., Vogt S., Xue S., Herzog G. F., Begemann F., Weber H. W., Middleton R., Fink D., and Klein J. 2000. Light noble gases and cosmogenic radionuclides in Estherville, Budulan and other mesosiderites: Implications for exposure histories and production rates. *Meteoritics & Planetary Science* 35:975–968.
- Aylmer D., Bonanno V., Herzog G. F., Weber H., Klein J., and

- Middleton R. 1988. ^{26}Al and ^{10}Be production rates in iron meteorites. *Earth and Planetary Science Letters* 88:107–118.
- Begemann F., Vilcsek E., Nyquist L. E., and Signer P. 1970. The exposure history of the Pitts meteorite. *Earth and Planetary Science Letters* 9:317–321.
- Begemann F., Weber H. W., Vilcsek E., and Hintenberger H. 1976. Rare gases and ^{36}Cl in stony iron meteorites: Cosmogenic elemental production rates, exposure ages, diffusion losses and thermal histories. *Geochimica et Cosmochimica Acta* 40:353–368.
- Bogard D. D., Burnett D. S., and Wasserburg G. J. 1969. Cosmogenic rare gases and the ^{40}K - ^{40}Ar age of the Kodaikanal iron meteorite. *Earth and Planetary Science Letters* 5:273–281.
- Bottke W. F., Nolan M. C., Melosh H. J., Vickery A. M., and Greenberg R. 1996. Origin of the Spacewatch small Earth-approaching asteroids. *Icarus* 122:406–427.
- Bottke W. F., Rubincam D. P., and Burns J. A. 2000. Dynamical evolution of main belt meteoroids: Numerical simulations incorporating planetary perturbations and Yarkovsky thermal forces. *Icarus* 145:301–331.
- Buchwald V. F. 1975. *Handbook of iron meteorites*. Berkeley: University of California Press. 1418 p.
- Burbine T. H., McCoy T. J., Meibom A., Gladman B., and Keil K. 2002. Meteoritic parent bodies: Their number and identification. In: *Asteroids III*, edited by Bottke W. F. Jr., Cellino A., Paolicchi P. and Binzel R. P. Tucson: The University of Arizona Press. pp. 653–667.
- Casanova I., Keil K., and Newsom H. E. 1993. Composition of metal in aubrites: Constraints on core formation. *Geochimica et Cosmochimica Acta* 57:675–682.
- Chang C. and Wänke H. 1969. Beryllium-10 in iron meteorites, their cosmic-ray exposure and terrestrial ages. In *Meteorite research*, edited by Millman P. Dordrecht, The Netherlands: Reidel. pp. 397–406.
- Cobbs J. C. 1966. Iron meteorites with low cosmic-ray exposure ages. *Science* 151:1524.
- Davis J. C., Proctor I. D., Southon J. R., Caffee M. W., Heikkinen D. W., Roberts M. L., Moore T. L., Turteltaub K. W., Nelson D. E., Loyd D. H., and Vogel J. S. 1990. LLNL/UC AMS facility and research program. *Nuclear Instruments and Methods in Physics Research B* 52:269–272.
- Farinella P., Vokrouhlicky D., and Hartmann W. K. 1998. Meteorite delivery via Yarkovsky orbital drift. *Icarus* 132:378–387.
- Fink D., Klein J., Middleton R., Vogt S., and Herzog G. F. 1991. ^{41}Ca in iron falls, Grant and Estherville: Production rates and related exposure age calculations. *Earth and Planetary Science Letters* 107:115–128.
- Gaffey M. J., Reed K. L., and Kelley M. S. 1992. Relationship of E-type Apollo asteroid 3103 (1982 BB) to the enstatite achondrite meteorites and the Hungaria asteroids. *Icarus* 100:95–109.
- Gladman B., Migliorini F., Morbidelli A., Zappala V., Michel P., Cellino A., Froeschle Ch., Levison H. F., Bailey M., and Duncan M. 1997. Dynamical lifetimes of objects injected into asteroid belt resonances. *Science* 277:197–201.
- Grady M. M. 2000. *Catalogue of meteorites*, 5th edition. London: The Natural History Museum. 690 p.
- Hartmann W. K., Farinella P., Vokrouhlicky D., Weidenschilling S. J., Morbidelli A., Marzari F., Davis D. R., and Ryan E. 1999. Reviewing the Yarkovsky effect: New light on the delivery of stone and iron meteorites from the asteroid belt. *Meteoritics & Planetary Science* 34:A161–A167.
- Herzog G. F., Lipschutz M. E., Jain A. V., and Rodman T. E. 1976. Noble gases and shock effects in the Odessa octahedrite. *Journal of Geophysical Research* 81:3583–3586.
- Herzog G. F., Vogt S., Albrecht A., Xue S., Fink D., Klein J., Middleton R., Weber H. W., and Schultz L. 1997. Complex exposure histories for meteorites with “short” exposure ages. *Meteoritics & Planetary Science* 32:413–422.
- Heymann D., Lipschutz M. E., Nielsen B., and Anders E. 1966. Canyon Diablo meteorite: Metallographic and mass spectrometric study of 56 fragments. *Journal of Geophysical Research* 71:619–641.
- Honda M., Nishiizumi K., Imamura M., Takaoka N., Nitoh O., Horie K., and Komura K. 1982. Cosmogenic nuclides in the Kirin chondrite. *Earth and Planetary Science Letters* 57:101–109.
- Honda M., Caffee M. W., Miura Y. N., Nagai H., Nagao K., and Nishiizumi K. 2002. Cosmogenic nuclides in the Brenham pallasite. *Meteoritics & Planetary Science* 37:1711–1728.
- Lavielle B., Marti K., and Regnier S. 1985. Exposure ages of iron meteorites: Complex histories and the constancy of galactic cosmic rays. In *Isotopic ratios in the solar system*. Toulouse, France: Cepadues Editions. pp. 15–20.
- Lavielle B., Marti K., Jeannot J.-P., Nishiizumi K., and Caffee M. 1999. The ^{36}Cl - ^{36}Ar - ^{40}K - ^{41}K records and cosmic ray production rates in iron meteorites. *Earth and Planetary Science Letters* 170:93–104.
- Leya I., Lange H.-J., Neumann S., Wieler R., and Michel R. 2000. The production of cosmogenic nuclides in stony meteoroids by galactic cosmic ray particles. *Meteoritics & Planetary Science* 35:259–286.
- Leya I., Neumann S., Wieler R., and Michel R. 2001. The production of cosmogenic nuclides by galactic cosmic ray particles for 2π exposure geometries. *Meteoritics & Planetary Science* 36:1547–1561.
- Lorenzetti S., Eugster O., Busemann H., Marti K., Burbine T. H., and McCoy T. 2003. History and origin of aubrites. *Geochimica et Cosmochimica Acta* 67:557–571.
- Magri C., Nolan M. C., Ostro S. J., and Giorgini J. D. 2007. A radar survey of main-belt asteroids: Arecibo observations of 55 objects during 1999–2003. *Icarus* 186:126–151.
- Masarik J. and Reedy R. C. 1994. Effects of bulk composition on nuclide production processes in meteorites. *Geochimica et Cosmochimica Acta* 58:5307–5317.
- Masarik J., Nishiizumi K., and Reedy R. C. 2001. Production rates of helium-3, neon-21, and neon-22 in ordinary chondrites and the lunar surface. *Meteoritics & Planetary Science* 36:643–650.
- Melosh H. J. 1984. Impact ejection, spallation, and the origin of meteorites. *Icarus* 59:234–260.
- Morbidelli A. and Gladman B. 1998. Orbital and temporal distributions of meteorites originating in the asteroid belt. *Meteoritics & Planetary Science* 33:999–1016.
- Nagai H., Honda M., Imamura M. and Kobayashi K. 1993. Cosmogenic ^{10}Be and ^{26}Al in metal, carbon and silicate of meteorites. *Geochimica et Cosmochimica Acta* 57:3705–3723.
- Nishiizumi K. 1995. Terrestrial ages of meteorites from cold and cold regions. In *Workshop on meteorites from cold and hot deserts*, edited by Schultz L., Annexstad J. O., and Zolensky M. E. LPI Technical Report #95–02. Houston, Texas: Lunar and Planetary Institute. pp. 53–55.
- Nishiizumi K. 2004. Preparation of ^{26}Al AMS standards. *Nuclear Instruments and Methods in Physics Research B* 223–224:388–392.
- Nishiizumi K., Imamura M., and Honda M. 1979. Cosmic ray produced radionuclides in Antarctic meteorites. *Memoirs of National Institute of Polar Research, Special Issue* 12:161–177.
- Nishiizumi K., Caffee M. W., and DePaolo D. J. 2000. Preparation of ^{41}Ca AMS standards. *Nuclear Instruments and Methods in Physics Research B* 172:399–403.
- Nishiizumi K., Imamura M., Caffee M. W., Southon J. R., Finkel R. C., and McAninch J. 2007. Absolute calibration of ^{10}Be AMS standards. *Nuclear Instruments and Methods in Physics Research B* 258:403–413.

- Olsen E., Davis A., Clarke, R. S. Jr., Schultz L., Weber H. W., Clayton R., Mayeda T., Jarosewicz E., Sylvester P., Grossman L., Wang M.-S., Lipschutz M. E., Steele I. M., and Schwade J. 1994. Watson: A new link in the IIE iron chain. *Meteoritics* 29:200–213.
- Ostro S. J., Campbell D. B., Chandler J. F., Hine A. A., Hudson R. S., Rosema K. D., and Shapiro I. I. 1991. Asteroid 1986 DA: Radar evidence for a metallic composition. *Science* 252:1399–1404.
- Rivkin A. S., Howell E. S., Lebofsky L. A., Clark B. E., and Britt D. T. 2000. The nature of M-class asteroids from 3- μ m observations. *Icarus* 145:351–368.
- Rubincam D. P. 1995. Asteroid orbit evolution due to thermal drag. *Journal of Geophysical Research* 100:1585–1594.
- Schaeffer O. A. and Heymann D. 1965. Comparison of ^{36}Cl - ^{36}Ar and ^{39}Ar - ^{38}Ar cosmic-ray exposure ages of dated fall iron meteorites. *Journal of Geophysical Research* 70:215–224.
- Schultz L. 1967. Tritium loss in iron meteorites. *Earth and Planetary Science Letters* 2:87–89.
- Sharma P., Kubik P. W., Fehn U., Gove G. E., Nishiizumi K., and Elmore D. 1990. Development of ^{36}Cl standards for AMS. *Nuclear Instruments and Methods in Physics Research B* 52:410–415.
- Tedesco E. F. and Gradie J. 1987. Discovery of M-class objects among the near-Earth asteroid population. *The Astronomical Journal* 93:738–746.
- Terribilini D., Eugster O., Mittlefehldt D. W., Diamond L. W., Vogt S., and Wang D. 2000. Mineralogical and chemical composition and cosmic-ray exposure history of two mesosiderites and two iron meteorites. *Meteoritics & Planetary Science* 35:617–628.
- Vilcek E. and Wänke H. 1961. Das Strahlungsalter der Eisenmeteorite aus Chlor-36 Messungen. *Zeitschrift für Naturforschung* 16a:379–384.
- Voshage H. and Feldmann H. 1979. Investigations on cosmic-ray produced nuclides in iron meteorites, 3. Exposure ages, meteoroid sizes and sample depths determined by mass spectrometric analyses of potassium and rare gases. *Earth and Planetary Science Letters* 45:293–308.
- Voshage H., Feldmann H., and Braun O. 1983. Investigations on cosmic-ray produced nuclides in iron meteorites: 5. More data on the nuclides of potassium and noble gases, on exposure ages and meteoroid sizes. *Zeitschrift für Naturforschung* 38a:273–280.
- Wasson J. T. and Wai C. M. 1970. Composition of metal, schreibersite, and perryite of enstatite achondrites and the origin of enstatite chondrites and achondrites. *Geochimica et Cosmochimica Acta* 34:169–184.
- Welten K. C., Caffee M. W., Leya I., Masarik J., Nishiizumi K., and Wieler R. 2003. Noble gases and cosmogenic radionuclides in the Gold Basin L4-chondrite shower: Thermal history, exposure history and pre-atmospheric size. *Meteoritics & Planetary Science* 38:157–173.
- Welten K. C., Nishiizumi K., Hillegonds D. J., Caffee M. W., and Masarik J. 2004. Unraveling the exposure histories of aubrites. *Meteoritics & Planetary Science* 39:A113.
- Wetherill G. W. 1985. Asteroidal source of ordinary chondrites. *Meteoritics* 20:1–22.
-